

Analysis of the Surface Drift Currents in the Bothnian Sea

Juha Uotila¹, Jouko Launiainen¹ and Timo Vihma²

¹ Finnish Institute of Marine Research, P.O.Box 33, FIN-00931, Helsinki, Finland

² Department of Geophysics, P.O. Box 4, FIN-00014, University of Helsinki, Finland

(Received: August 1994; Accepted: January 1995)

Abstract

Surface drift in the eastern part of the Bothnian Sea was studied by using satellite-tracked buoys. Two drifter experiments were performed during the Gulf of Bothnia Year 1991 in June and November. Both experiments were carried out near the Finnish coast and the buoy clusters drifted northwards almost parallel to the coastline. The dominant wind was from southeast to southwest. The mean drift speed in June and November was 10 cm/s and 14 cm/s and the mean geostrophic wind velocities were 6 m/s and 11 m/s, respectively. In the June experiment dispersion characteristics were more obvious than in the November experiment. In June an inertial-type motion was found at the period of about 13.9 h. Geostrophic surface wind fields were calculated from two different pressure analyses, one given by the HIRLAM and another by the ECMWF. A numerical interpolation method was used to define the geostrophic wind for the buoy site. Linear relationships between the wind and the buoy centroid drift speed were studied. Wind was the most remarkable factor generating the surface drift, but coastal and topographical effects were of importance as well. The latter effects were seen in the turning angle between the direction of the geostrophic wind and the drift. The drift speed was of 0.8-1.2 % of the geostrophic wind speed and was directed on the average some 30° left of the wind direction.

Key words: oceanography, surface drift, geostrophic wind

1. Introduction

The Gulf of Bothnia Year 1991 project was a programme aiming at a better knowledge of the environmental and ecological system of the northern part of the Baltic Sea. The project included also a physical sub-programme for studies of currents and hydrography in the Bothnian Sea. The sub-programme was carried out jointly by Finnish, Swedish and Canadian teams. Coastal-open sea exchange and currents were investigated using moored current meters and satellite-tracked drifting buoys. The preliminary results of the physical programme have been presented by *Murthy et al.* (1993).

Two drifter experiments were carried out near the Finnish coast in June and November 1991, when eight separate drifters were deployed from *R/V Aranda* (Fig. 1). The primary goal of the Finnish drifter experiments was to improve knowledge of the water drift and dispersion in the eastern Gulf of Bothnia (*Launiainen et al.*, 1993). In the northwest part of the Bothnian Sea similar drifter experiments as the Finnish experiments

were carried out by the Swedish team (*Håkansson and Rahm, 1993*). The difference between summer conditions of weak wind and strong thermal stratification and autumnal strong wind conditions was one point of interest. Additionally, further insight to spatial and temporal variations of the surface currents in the area was expected to be achieved when using both drifter and current meter data.

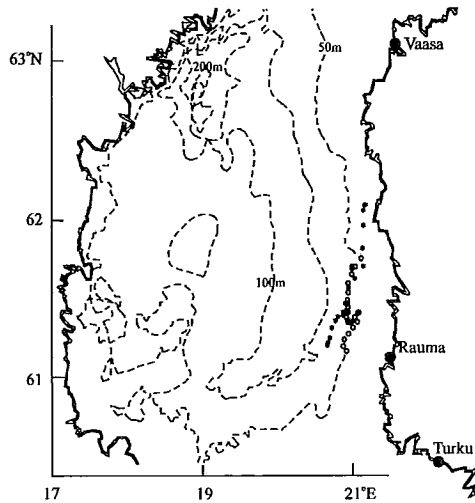


Fig. 1. Finnish drifter experiments in the Gulf of Bothnia Year 1991. June experiment with circles (o) and November experiment with asterisks (*). Buoy cluster centroid positions plotted at 12-hour intervals.

The Bothnian Sea is a relatively restricted basin between Finland and Sweden. The bottom topography is characterized by the difference between more regular Finnish part and deeper and quite irregular Swedish part of the basin. The eastern part of the Bothnian Sea is mostly open sea where the depth decreases gradually from over 100 m in the offshore towards the coast (Fig. 1). The average current field in the Bothnian Sea have been studied by *Palmén (1930)*. He found that the long-term average flow pattern is characterized by a large cyclonic vortex. The stability of the vortex, however, is weak, only 20-30 %, because of the wind fluctuations. Accordingly, the wind plays a significant role in generating currents in the Bothnian Sea.

2. Observations

General drift characteristics

Two different buoy types were used (Fig. 2a and Fig. 2b) in both experiments. Both buoy types had a similar drogue, but they had different kind of surface floats. Eight buoys (four of each type) drifted in the first experiment from 3 to 18 June 1991 and in the second experiment from 5 to 16 November 1991. The buoys were equipped with rectangular

drogues installed at 5 m depth. The floating part of the buoy-system contained the electronics and the transmission antenna for the satellite positioning. The CLS Argos system was used to locate buoy trajectories and the location accuracy was given in three categories: 1 km, 350 m and 150 m (*Launiainen et al.*, 1993). The middle category was the most common and the type-a buoys showed a better behaviour in both experiments than the type-b ones. In the June experiment the Argos system located one buoy on the average 17.3 times per day and in November 13.7 times per day. The location accuracy of the Argos system was studied in more detail by *Launiainen et al.* (1991).

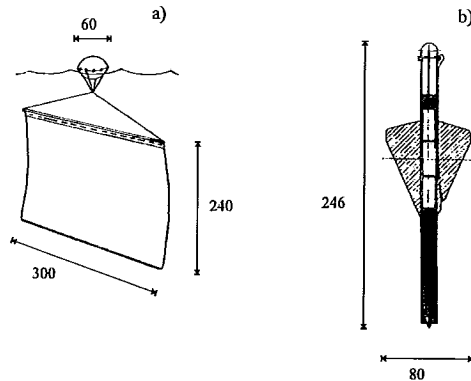


Fig. 2. Buoy types (dimensions in cm). The drogue for the type (b) buoy (Christian Michelsen Research, Norway) is the same as for the type (a) buoy (Hermes Electronics Inc., Canada).

From the various buoy trajectories the centroid (centre of population) was calculated. All buoys were assumed to have the same dynamical properties and the centroid trajectory was the arithmetic mean of the separate buoy positions. Individual buoy trajectories and centroid trajectories can be seen in Fig. 3. During both experiments the buoys drifted almost parallel to the coastline. However, in the November experiment buoys were deployed further from the coast than in June, but recovered from shallower water. The buoys also drifted a longer distance in a shorter time during the autumn experiment compared to the summer case. These differences are caused by the differences in wind conditions and seasonal variations in the atmospheric and the aqueous boundary layers.

Dispersion characteristics during the experiments were also studied. In the June experiment the buoy drift was more diffusive than in November (Fig. 3). Assuming along-axis and transversal dispersion as equal, the diffusivity i.e. rate of dispersion when determined from $K_D = (d\delta^2/dt)/2$, where K_D is the diffusivity and d/dt means a derivation with respect of time and δ^2 is the variance of buoy distances from the centroid (*Csanady*, 1973), yields for June and November values of $4.5 \cdot 10^5 \text{ cm}^2/\text{s}$ and $2.0 \cdot 10^4 \text{ cm}^2/\text{s}$, respectively. The dispersion in June was one order of magnitude larger than in November. However, diffusivities of these buoy experiments are smaller than measured from oceanic mesoscale eddies, where dispersion rates can be of $10^7 \text{ cm}^2/\text{s}$ (*de Verdiere*, 1983).

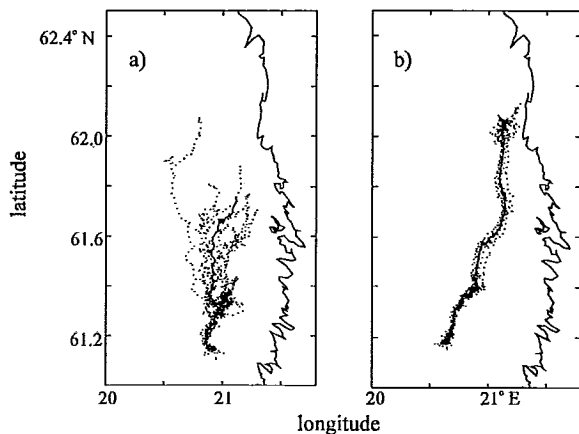


Fig. 3. Drift trajectories of the various buoys. (a) June experiment and (b) November experiment. Trajectory of centroid is given with solid line.

Drift velocities were calculated from 6-hour and 1-hour interpolated locations. According to *Vihma and Launiainen* (1993), the 6-hour interpolated drift velocities were considered to include the major part of small-scale dynamics, but not significant pseudo-movements due to location errors. Rotary velocity spectra of the drift based on an algorithm given by *Thorndike* (1986) were calculated from 1-hour interpolated velocities. During the June experiment an inertial-type motion was observed in the clockwise spectrum at the period of about 13.9 h (Fig. 4).

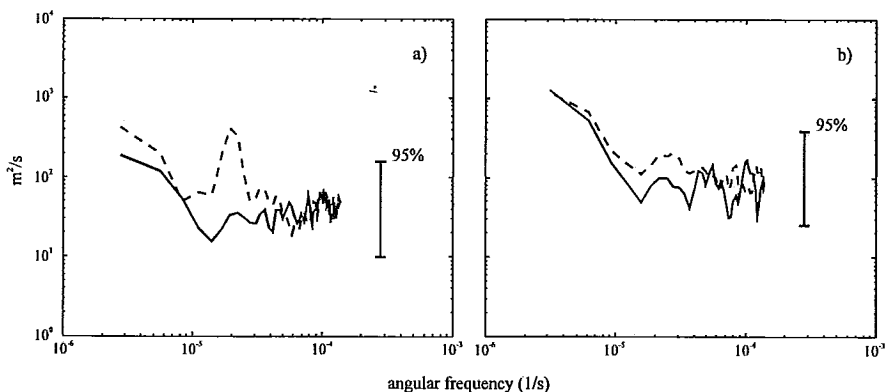


Fig. 4. Drift velocity rotary spectra of June experiment (a) and November experiment (b). The anticlockwise spectra are given with solid line and the clockwise with dashed line.

Pressure analyses and the geostrophic wind

The geostrophic surface wind field was calculated from the surface pressure analyses given by the High Resolution Limited Area Model (HIRLAM) and by the European Centre for Medium-Range Weather Forecasts (ECMWF). The HIRLAM-analyses were available for the study in graph form only, but the ECMWF-analyses were in numeric form and therefore the ECMWF-analyses were to some extent spatially more accurate. The HIRLAM-analyses time interval was 6-hour and the ECMWF 12-hour (Table 1). From Table 1 can be seen that the spatial resolution of the HIRLAM-analysis was remarkably lower than that of the ECMWF-analysis particularly in the longitude direction because of the graphic origin of the data. Geostrophic winds at buoy sites were calculated from pressure gradients (as $u_g = -(1/\rho f)(\partial p/\partial y)$, $v_g = (1/\rho f)(\partial p/\partial x)$ where ρ is the air density and f is the Coriolis parameter) by a two-step numerical interpolation method. For the first step, the air pressure values were interpolated around the buoy location by the second-degree Taylor series so that the second-degree pressure gradient approximation was available for the second step. A detailed description of the method is given by *Uotila* (1994).

Table 1. Properties of the pressure analyses.

Grid property	HIRLAM	ECMWF
size (width x height)	3 x 4	15 x 11
resolution (width / height)	6° / 1°	0.5° / 0.5°
area	14.0° - 26.0°E 60.5° - 63.5°N	16.0° - 23.0°E 59.5° - 64.5° N
interval	6 hours	12 hours

During the June experiment the wind was mainly from southeast to southwest (Fig. 5a). At the beginning of the period the wind came from southeast and then turned to southwest. In the middle of the period the wind was weaker, but it strengthened again towards the end. During the November experiment the wind was stronger than in June (Fig. 5b). The wind direction mainly varied between southeast and southwest, but around the 314 Julian day it temporally turned to northwest. An apparent similarity between the drift and the wind vectors can be seen by comparing the time series for both quantities in Fig. 5.

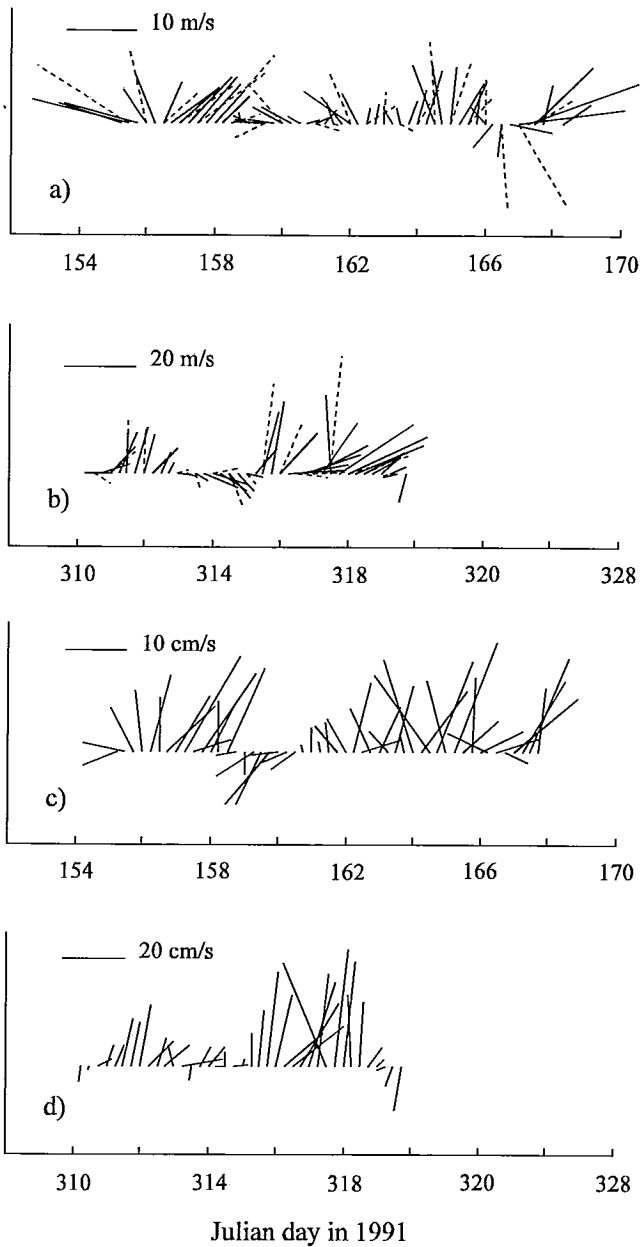


Fig. 5. Vectors of the geostrophic wind calculated from the pressure analyses and the drift velocity vectors of the buoy centroid in the both experiments. In (a) and (b) the geostrophic surface wind based on the HIRLAM pressure analyses given as solid and the one based on the ECMWF pressure analyses as dashed line (observed where the wind goes). (a) and (c) for June experiment, and (b) and (d) for November experiment. The time interval between the velocity vectors is 6 hours.

3. Relationship between the drift and the wind

The dependence of the 6-hour interpolated drift velocity on the geostrophic wind was analysed. A linear relationship between the wind and the drift was assumed as a first approximation. A model of this kind was presented by *Kirwan and Cresswell* (1982) for the relationship between the drift and the surface boundary layer wind velocities. A standard statistical model of the form

(1)

was applied for the time series of the velocity components. The subscripts d and g refer to the drift speed and the geostrophic wind speed, respectively. The regression coefficients a_{ij} and the residual terms u_{res} and v_{res} can be computed by the least square method, and they were determined for two different kind of cases (cf. *Kirwan and Cresswell*, 1982). The first was the general case in which each of the a_{ij} was taken as independent. Accordingly, the general case model can be presented in matrix form of

$$\mathbf{V}_d = \mathbf{U}_g \alpha + \mathbf{V}_{res} \quad (2)$$

The second case was the more discrete one i.e. the commonly used two-parameter case in which $a_{11}=a_{22}=b_1$ and $a_{12}=-a_{21}=b_2$. This case allows a constant speed ratio and a constant angle between the drift and the wind vector. If velocity vectors are assumed to be complex variables the two-parameter case is the most general linear relationship between the drift and the wind. The two-parameter case model can be presented thus in the complex form

$$\mathbf{V}_d = \mathbf{U}_g \beta + \mathbf{V}_{res} \quad (3)$$

where β is a complex variable with the real part b_1 and the imaginary part b_2 . The speed ratio r and the angle φ between the drift and the wind vectors can be calculated from the eq. (4).

$$\begin{cases} r = \sqrt{b_1^2 + b_2^2} \\ \varphi = \arctan(b_2/b_1) \end{cases} \quad (4)$$

If $b_1=b_2$ is assumed, the two-parameter case corresponds to the classical theory of Ekman wind-drift currents (*Ekman*, 1905). According to *Kirwan and Cresswell* (1982), the boundary layer theory gives a linear relationship between the drift and surface wind

velocities. If surface wind data is used instead of the geostrophic surface wind in eq. (1), the residual terms represent the sea surface residual current. If the linear relationship between the drift and geostrophic wind is assumed, residual terms include also a non-linear portion between the geostrophic and surface winds.

The dependence of the speed ratio and the turning angle between the drift and the geostrophic wind during the drifter experiments are presented in Fig. 6. With stronger winds scattering of the speed ratio decreases and approaches stationary values as can be seen from Fig. 6a. This shows clearly that the speed ratio can not be assumed constant under conditions of weak unstationary winds. However, near the coast the basin's topography guides the drift. Thus, outside the coastal zone it is reasonable to think that the surface drift response to the wind is independent of wind direction. In this area the general case model and the two-parameter case model are supposed to give more similar results than near the coastline. When the wind has a component towards the shore, the data suggest that the surface drift remains almost parallel to the coastline although the wind turns against the coast (see Fig. 6b). When the wind blows away from the coast no evident dependence between the turning angle and the geostrophic wind direction appears. In Fig 6b non-stationary wind observations (the difference between successive wind directions was more than $\pm 45^\circ$) and wind magnitudes less than 7 m/s were not considered.

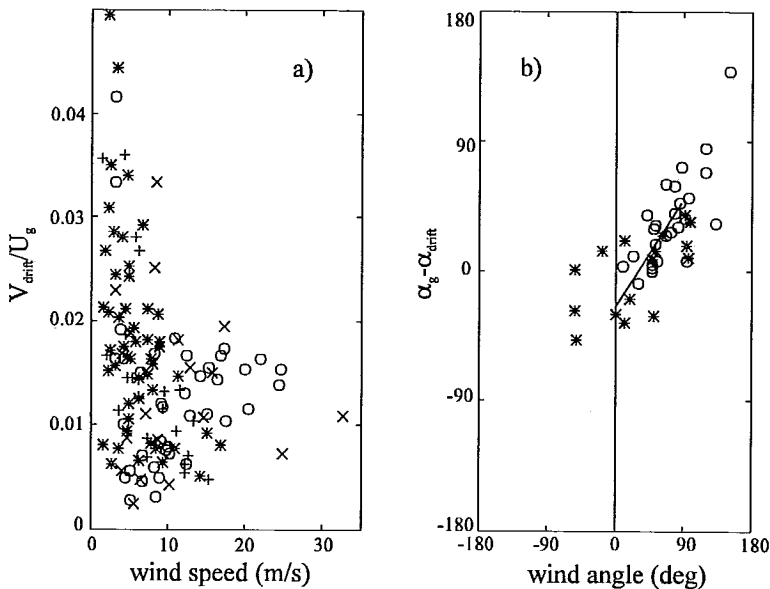


Fig. 6. (a) Drift speed of the buoy centroid with respect to the geostrophic wind speed, versus the geostrophic wind speed. (b) Turning angle between the direction of the geostrophic wind and the drift, versus the direction of geostrophic wind. For the wind angle, 0, 180, and -180 correspond to the alongshore winds. If the wind velocity has a component towards the coast, the wind angle is positive. Symbols: HIRLAM winds in June (*) and in November (o) and, ECMWF winds in June (+) and in November (x).

The time averages of residual terms according to equations (2) and (3) are presented in Table 2 for both cases. Unfortunately, the observation periods were quite short for a representative statistical analysis. The values from Table 2 for the general case are smaller than for the two-parameter case, because the general case explains more variation than the two-parameter case. The residual velocity vectors point mainly northwards, which is in accordance with results of *Palmén* (1930), who estimated a residual current of 2.5 cm/s to the north in the area. However, the residual velocity vectors can vary widely and neither apparent direction nor magnitude appears from the data. In Table 3 the speed ratio and the turning angle between the drift and the geostrophic wind speed is presented for the two-parameter case calculated from eqs. (3) and (4). The speed ratio is about 1 %, which is to be expected, but from the turning angle values it can be seen that the coastal influence on the drift tends to be significant. According to earlier experiments (*McNally*, 1981; *Kirwan* and *Cresswell*, 1982), surface drifter trajectories point to the right of the isobars (geostrophic wind), when the large-scale wind-induced motion dominates and coastal effects are of no importance. In our case, however, the buoys drifted, on the average, 9°...34° to the left of the geostrophic wind.

Table 2. Time averages of residual terms (dimensions in cm/s) from eqs. (2) and (3).

Period	General case		Two-parameter case	
	$\langle u_{res} \rangle$	$\langle v_{res} \rangle$	$\langle u_{res} \rangle$	$\langle v_{res} \rangle$
HIRLAM June	-0.03	0.37	1.11	2.23
ECMWF June	0.82	2.87	1.55	3.26
HIRLAM November	0.30	-0.64	-0.67	1.45
ECMWF November	0.35	0.03	0.64	4.48

Table 3. The speed ratio r and the difference angle from eq. (4). Positive values indicate drift direction left from the wind.

Period	r (%)	φ (deg)
HIRLAM June	1.2	9
ECMWF June	0.8	34
HIRLAM November	1.2	34
ECMWF November	1.1	30

The correlation coefficients between simulated velocity components using the regression models and observations are given in Table 4. In the June experiment correlations of velocity components are quite good, but in November the cross-shore velocity component of regression models correlates worse with observations than the alongshore velocity component. This is due to stronger wind velocities towards the coast in November and the effect of the coastal zone, which turned the surface current parallel to the coastline. Mutual differences between the general case and the two-parameter case are not significant even in November when coastal effects were obvious. The two-parameter case explains nearly as much variance as the general case but with two less parameters. The HIRLAM-analyses give better correlations than the ECMWF-analyses though the spatial resolution of the HIRLAM was poor in this study. The HIRLAM is, however, a limited area model and has a better temporal resolution than the ECMWF.

Table 4. Correlation coefficients between the simulated and the observed velocity components.

Period	General case		Two-parameter case	
	u_d	v_d	u_d	v_d
HIRLAM June	0.71	0.73	0.69	0.73
ECMWF June	0.74	0.52	0.75	0.46
HIRLAM November	0.49	0.93	0.47	0.93
ECMWF November	0.51	0.88	0.51	0.76

Based on the regression parameters from eqs. (2) and (3) some simulations were made for comparing simulated centroid trajectories to the observed ones. Time steps in the simulations were 6- and 12-hours induced by the pressure analyses intervals. Four simulation examples are presented in Figs. 7 and 8. In Fig. 7 the drift has been simulated using the regression parameters calculated from the period to be studied. In June (Fig. 7a), both pressure analysis schemes simulate rather well the observed trajectory, but in November (Fig. 7b) the simulated drift goes more rapidly northwards. Linear regression models cannot therefore well explain the coastal zone effect. Additionally, trajectories in November are more difficult to simulate with used time steps than in June because stronger winds are resulting in stronger drift velocities. Simulations were also done by parameters calculated from other periods than to be simulated. These cross period simulations are illustrated in Fig. 8. Using parameters of the November experiment for June (Fig. 8a) causes the turning of simulated trajectories away from the coast westwards. On the contrary, when using June parameters in November (Fig. 8b) simulations gives unrealistic drift towards the coast. This implies that especially in the November experiment the coastal response to the drift is significant and affects also the values of the regression parameters.

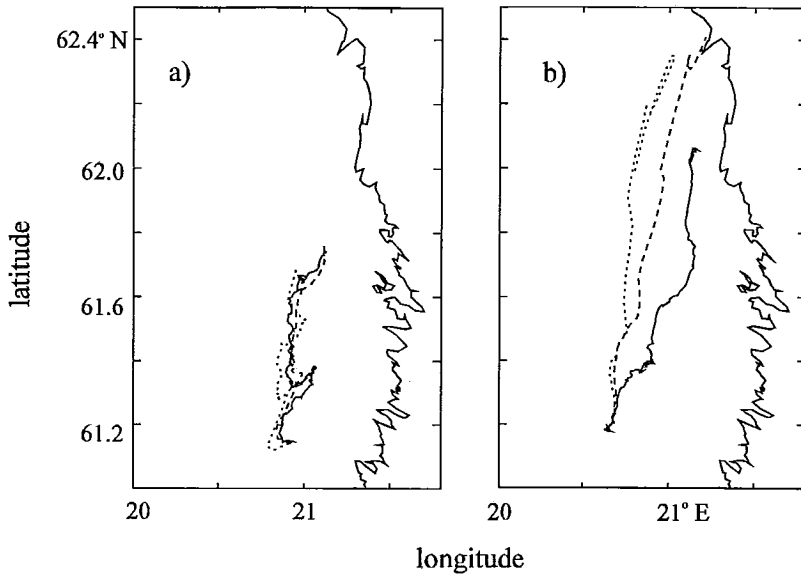


Fig. 7. Two general case drift simulations, (a) for June and (b) for November. The solid line gives the observed trajectory of the centroid. The dashed line gives the simulated trajectory with the HIRLAM winds and the dotted line gives the one with the ECMWF winds.

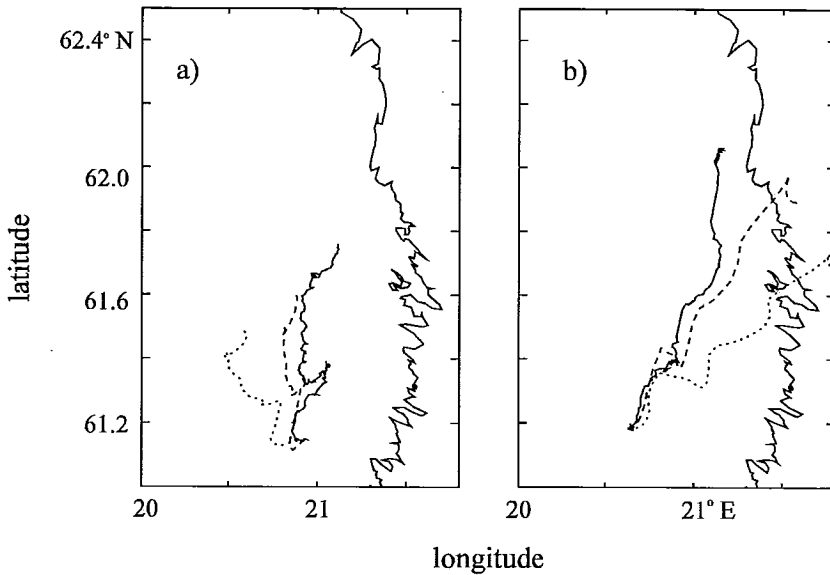


Fig. 8. Two cross period drift simulations with the HIRLAM winds. (a) for June using the regression parameters obtained for November and (b) for November using the parameters obtained for June. The solid line gives the observed trajectory of the centroid. The dashed line gives the general case trajectories and the dotted line gives the two-parameter case trajectories.

4. Concluding remarks

The Gulf of Bothnia Year 1991 surface drifter experiments were studied with respect to the geostrophic wind, based on two pressure analysis schemes. Even though the correlation between the drift and the wind was significant, the effect of the coast and bottom topography was obvious, especially during the autumnal experiment. In addition, an inertial-type of motion was detected during the June experiment when light winds occurred.

Effects of the structure of the atmospheric and the aqueous boundary layer on the drift was not analyzed, but usually one can assume these to be significant. The atmospheric boundary layer controls the relationship between the geostrophic wind and the momentum flux from air to the sea, and the stratification of the water column determines how the momentum flux will spread through the water mass, controlling the current structure. Because of an apparent non-linear relationship between the geostrophic and the surface wind, the linear regression model was not able to separate the wind-induced part of the observed sea surface current. On the other hand, the local surface wind fields were difficult to construct because of the lack of on-site meteorological observations.

The present study concentrated mostly on the study of the centroid trajectories, but the dispersion characteristics of the drift were quite different during the experiments. Combining the Swedish and Finnish drifter data, further insight into the dispersion characteristics of the drift may be considered in future analysis. Currently, the methodology used in this study, is being used for our recent experiments carried out in the Gulf of Finland, in the Denmark Strait and in the Weddell Sea.

Acknowledgments

The work was financially supported by the Gulf of Bothnia Year 1991 project, which is gratefully acknowledged.

5. References

- Csanady, G. T., 1973: *Turbulent Diffusion in the Environment*, D. Reidel Publishing Company, Dordrecht, 249 pp.
- Ekman, V. W., 1905: On the Influence of the Earth's Rotation on Ocean Currents, *Arkiv för Matematik, Astronomi, och Fysik*, 2, No. 11, pp. 1-52.
- Kirwan, A. D. and Cresswell, G. R., 1982: Observations of Large and Mesoscale Motions in the Near-Surface Layer, in *Proceedings of the International School of Physics "Enrico Fermi"; Course LXXX*, North-Holland Publishing Company, Amsterdam, pp. 79-125.
- Håkansson, B. and Rahm, L., 1993: Swedish Lagrangian Current Experiments, in *The Gulf of Bothnia Year-1991, Physical transport experiments*, RO 15, SMHI Reports Oceanography, Norrköping, pp. 41-54.

- Launiainen, J., T. Vihma, J. Aho and Rantanen, K., 1991: Air-Sea Interaction Experiment in the Weddell Sea, Argos-Buoy Report from FINNARP-5/89, 1990-1991, *Antarctic Reports in Finland, Report No.2*, Ministry of Trade and Industry, Helsinki.
- Launiainen, J., T. Stipa, H. Grönvall and Vihma, T., 1993: Finnish Lagrangian Current Experiments, in *The Gulf of Bothnia Year-1991, Physical transport experiments*, RO 15, SMHI Reports Oceanography, Norrköping, pp. 55-66.
- McNally, G. J., 1981: Satellite-Tracked Drift Buoy Observations of the Near-Surface Flow in the Eastern Mid-Latitude North Pacific, *J. Geophys. Res.*, **86**, 8022-8030.
- Murthy, R., B. Håkansson and Alenius, P., 1993: Editors in *The Gulf of Bothnia Year-1991, Physical Transport Experiments*, RO 15, SMHI Reports Oceanography, Norrköping, 127 p.
- Palmén, E., 1930: Untersuchungen über die Strömungen in den Finnland umgebenden Meeren, *Soc. Scient. Fenn., Comm. Phys.-Math.*, **V. 12.**, pp. 1-41.
- Thorndike, A. S., 1986: Kinematics of Sea Ice, in Untersteiner N. (ed.): *The Geophysics of Sea Ice*, Plenum Press, New York, pp. 489-549.
- Uotila, J., 1994: Ajopojujen ajelehtimisesta Selkämerellä Pohjanlahtivuonna 1991 [Analysis of the buoy drift in the Bothnian Sea during the Gulf of Bothnia Year 1991], *Merentutkimuslaitos. Sisäinen raportti 1994 (7)*, Helsinki, 83 p (In Finnish).
- de Verdiere, A. C., 1983: Lagrangian eddy statistics from surface drifters in the eastern North Atlantic, *J. Mar. Res.*, **41**, 375-398.
- Vihma, T., and Launiainen, J., 1993: Ice Drift in the Weddell Sea in 1990-1991 as Tracked by a Satellite Buoy, *J. Geophys. Res.*, **98**, 14, 471-14,485.